Analysis of Nonlinear Elastic Membrane Oscillations by Eigenfunction Expansion

Andras Balogh and Vladimir Varlamov
Department of Mathematics
The University of Texas-Pan American
Edinburg, TX 78539
USA

Abstract: - In this paper we examine a spatially two–dimensional forced, damped Boussinesq equation with quadratic nonlinearity. This equation describes small, nonlinear oscillations of a circular, elastic membrane in the presence of viscosity. The eigenfunction expansion method is used for the purpose of constructing solutions for small initial data analytically. The constructive method enables us to perform numerical simulations as well. The conservative theoretical results are extended through numerical simulations: we examine the convergence properties, the smallness requirement on the perturbation parameter, and the long–time behavior of the system.

Key-Words: - Numerical simulation, Boussinesq equation, Eigenvalue expansion, Quadratic nonlinearity.

1 Introduction

Membrane structures have been used since the earliest of times. However, in the past their analysis has relied mostly on trial and error, while modern analysis provides powerful tools for creating mathematical theory of description of their motions. The deformations of these structures are essentially nonlinear. Nevertheless the linear theory provides an important starting point for understanding this complicated behavior.

The first membrane structures were biological organisms which probably represent the widest usage of this structure type [3]. Examples range from dragonfly and bat wings to the bullfrog's inflatable throat [4]. Investigations of biomechanics of flexible membranes is a current activity.

The necessity of creation of passive sensor technologies determines the importance of study of oscillations of elastic membranes. Unattended ground sensors can have as their basic element a circular membrane with fixed ends (clamped, simply supported or even nonlinearly damped). Circular geometry is not the only option, geometric optimization (shape or form finding) is one of the two main branches of research in this area, the other one being response analysis. The latter represents the topic of the present investigation.

Although all processes in the nature are eventually nonlinear, small perturbations of thin elastic plates in "normal conditions" can be often described in the framework of linear models. However extreme weather conditions like intense heat, high humidity etc. can increase the influence of nonlinearity, i.e., make the behavior of the membrane "more nonlinear" than in normal conditions [9]. That is to say nothing of the change of amplitude of the incident external perturbation which may also provoke essentially nonlinear response. All this is quite relevant to our primary interest in the models describing acoustic detection via registration of membrane oscillations.

2 Problem Statement and Main Results

The so called "good" Boussinesq equation is well known in the context of governing small nonlinear oscillations of elastic beams. This equation can be written in the form (see [14, 8])

$$u_{tt} + \alpha^2 u_{xxxx} = u_{xx} + \beta(u^2)_{xx}, \tag{1}$$

where $\alpha = const > 0$ is the dispersion parameter depending on the compression and rigidity characteristics of the material and β is the constant coefficient controlling nonlinearity (it can be set equal to one by appropriate scaling, but we will keep it in order to trace the influence of the nonlinearity). The quadratic nonlinearity appearing in (1) accounts for the curvature of the bending beam. In many practical situations damping effects are comparable in strength to nonlinear and dispersive ones and in such cases the model equation presented above requires a dissipative term [1]. One possibility is to introduce the so called internal damping term due to friction [14]. The equation becomes then

$$u_{tt} - 2bu_{txx} = -\alpha^2 u_{xxxx} + u_{xx} + \beta(u^2)_{xx}, \tag{2}$$

where $b = const > 0$ is the viscosity coefficient. Another possibility would be to replace the second term on the left–hand side by $-bu_t$ (usually called weak damping although the damping effect in fact depends on the frequency

of oscillations). Two–dimensional analog of equation (2) (sometimes called damped plate equation [6**?**]) appears in the context of modeling small nonlinear oscillations of elastic membranes. It can be written as

$$u_{tt} - 2b\Delta u_t = -\alpha^2\Delta^2 u + \Delta u + \beta\Delta(u^2). \tag{3}$$

Consider now the nonlinear analog of the model presented above with a forcing term $af(r,\theta,t)$ due to acoustic pressure. In order to simplify some considerations we consider now the simply supported edge of the membrane (see [7]). We can pose the problem for the vertical deflection of the plate u as follows

$$\begin{gathered} u_{tt} - 2b\Delta u_t = -\alpha\Delta^2 u + \Delta u + \beta\Delta(u^2) + af(r,\theta,t), \\ u|_{\partial\Omega} = \Delta u|_{\partial\Omega} = 0, \\ u(r,\theta,0) = u_t(r,\theta,0) = 0, \\ u(r,\theta+2\pi,t) = u(r,\theta,t), \\ \text{for } (r,\theta) \in \Omega,\ t > 0 \\ \text{boundedness of } u \text{ at the origin,} \end{gathered} \tag{4}$$

where α, b and a are positive constants, β is a real constant, Ω denotes the unit disk, and $\partial\Omega$ is its boundary, the unit circle. The parameter a controls the forcing term and must be bounded in order to guarantee convergence of a certain series. Therefore acoustic pressure is expected to be not too big in the framework of the current model. Large nonlinear oscillations will be considered in the future. We consider the case when the edge of the disk is clamped. Paper [11] dealt with the nonlinear beam oscillations for the case of simply supported ends (one–dimensional case) and in [12] nonlinear oscillations of an elastic ball (three–dimensional case) were studied in the framework of the same Boussinesq model.

We restrict our attention to the most interesting case $\alpha^2 > b^2$ of small damping which corresponds to the existence of an infinite number of damped oscillations. If the inverse relation holds (the so called overdamping case), aperiodic processes play the main role.

We seek solutions of the problem (4) in the form of the eigenfunction expansion

$$u(r,\theta,t) = \sum_{m=-\infty}^{\infty}\sum_{n=1}^{\infty} \hat{u}_{mn}(t)\Phi_{mn}(r,\theta) \tag{5}$$

where

$$\Phi_{mn}(r,\theta) = J_m(\lambda_{mn}r)e^{im\theta}, \quad m \in \mathbb{Z},\ n \in \mathbb{N} \tag{6}$$

are eigenfunctions of the Laplace operator in a disk, i.e. solutions to the eigenvalue problem

$$\begin{gathered} \Delta\Phi(r,\theta) = -\Lambda\Phi(r,\theta), \qquad (r,\theta) \in \Omega, \\ \Phi|_{\partial\Omega} = 0, \quad \Phi(r,\theta+2\pi) = \Phi(r,\theta), \\ |\Phi(0,\theta)| < \infty. \end{gathered}$$

In this way we can satisfy the boundary conditions, periodicity conditions in θ and the boundedness condition for u. The function J_m is the Bessel function of the first kind of order m for $m \in \mathbb{N}$. In order to satisfy the boundary conditions $\{\lambda_{mn}\}_{n=1}^{\infty}$ should be positive zeros of the dispersion equation

$$J_m(\lambda) = 0 \quad \text{for} m \in \mathbb{Z}.$$

Our choice of the boundary condition simplifies the dispersion relation. So far our approach resembles the classical method of separation of variables, but now the necessity to solve the nonlinear equation brings new ideas into consideration.

The sequence $\{\Phi_{mn}\}_{m\in\mathbb{Z},n\in\mathbb{N}}$ forms a complete orthogonal set in $L_2(\Omega)$. Expanding the source term of the equation into the series of the (5) type we obtain

$$f(r,\theta,t) = \sum_{m=-\infty}^{\infty}\sum_{n=1}^{\infty} \hat{f}_{mn}(t)\Phi_{mn}(r,\theta).$$

Using notation $\langle\cdot,\cdot\rangle$ and $\|\cdot\|$ for the L_2–inner product and norm respectively we have

$$\hat{f}_{mn}(t) = \frac{< f, \Phi_{mn} >}{\|\Phi_{mn}\|^2}, \tag{7}$$

and recalling the initial conditions for u we obtain the following nonlinear initial value problem for the coefficients $\hat{u}_{mn}(t)$:

$$\begin{gathered} \hat{u}''_{mn}(t) + 2b\lambda_{mn}^2\hat{u}'_{mn}(t) + (\alpha\lambda_{mn}^4 + \lambda_{mn}^2)\hat{u}_{mn}(t) \\ = -\beta\lambda_{mn}^2\widehat{u^2}_{mn}(t) + a\hat{f}_{mn}(t),\ t > 0, \\ \hat{u}_{mn}(0) = \hat{u}'_{mn}(0) = 0, \end{gathered} \tag{8}$$

where the coefficients of the eigenfunction expansion of the nonlinearity are calculated by the formulae

$$\begin{aligned} \widehat{u^2}_{mn}(t) &= \frac{< u^2, \Phi_{mn} >}{\|\Phi_{mn}\|^2} \\ &= \left\langle \sum_{p,q}\hat{u}_{pq}(t)\Phi_{pq} \cdot \sum_{k,s}\hat{u}_{ks}(t)\Phi_{ks}, \Phi_{mn} \right\rangle \\ &= \sum_{p,q,k,s} b(m,n;p,q,k,s)\hat{u}_{pq}(t)\hat{u}_{ks}(t), \end{aligned}$$

and

$$b(m,n,p,q,k,s) = \frac{< \Phi_{pq}\cdot\Phi_{ks}, \Phi_{mn} >}{\|\Phi_{mn}\|^2}. \tag{9}$$

Integrating (8) with respect to t we get the nonlinear integral equation

$$\begin{aligned} \hat{u}_{mn}(t) &= \frac{a}{\sigma_{mn}}\int_0^t e^{-b\lambda_{mn}^2(t-\tau)}\sin[\sigma_{mn}(t-\tau)]\,\hat{f}_{mn}(\tau)d\tau \\ &- \frac{\beta\lambda_{mn}^2}{\sigma_{mn}}\int_0^t e^{-b\lambda_{mn}^2(t-\tau)}\sin[\sigma_{mn}(t-\tau)]\,\widehat{u^2}_{mn}(\tau)d\tau, \end{aligned} \tag{10}$$

where

$$\sigma_{mn} = \lambda_{mn}\sqrt{k\lambda_{mn}^2 + 1} \text{ and } \qquad k = \alpha - b^2 > 0.$$

We apply the perturbation theory in order to solve (10). We seek the solution in the form

$$\hat{u}_{mn}(t) = \sum_{N=0}^{\infty} a^{N+1}\hat{v}_{mn}^{(N)}(t). \tag{11}$$

Substituting (11) into equation (10) we obtain the recursion formulas

$$\hat{v}_{mn}^{(0)}(t) = \frac{1}{\sigma_{mn}} \int_0^t e^{-b\lambda_{mn}^2(t-\tau)} \sin\left[\sigma_{mn}(t-\tau)\right] \hat{f}_{mn}(\tau) d\tau, \tag{12}$$

and

$$\hat{v}_{mn}^{(N)}(t) = -\frac{\beta\lambda_{mn}^2}{\sigma_{mn}} \int_0^t e^{-b\lambda_{mn}^2(t-\tau)} \sin\left[\sigma_{mn}(t-\tau)\right] \times \sum_{p,q,k,s} b(m,n,p,q,k,s) \sum_{j=1}^{N} \hat{v}_{pq}^{(j-1)}(\tau) \hat{v}_{ks}^{(N-j)}(\tau) d\tau \tag{13}$$

for $N \geq 1$.

Formulas (5), (9), (11), (13) provide the algorithm of computation of the vertical deflection u. In order to guarantee the absolute and uniform convergence of the series (9), parameter a should not exceed some critical value a_0 which is determined by the nonlinearity of the equation and the source term. The following estimate holds for the coefficients $\hat{v}_{mn}$:

$$\left|\hat{v}_{mn}^{(N)}(t)\right| \leq c^N (N+1)^{-2} \lambda_{mn}^{-3/2}, \tag{14}$$

where

$$c = \frac{1}{b} \sup_{t>0} \left|\hat{f}_{mn}(t)\right|. \tag{15}$$

Substituting estimate (14) into (11) we see that

$$a < 1/c \tag{16}$$

is a sufficient condition for convergence.

The following theorem summarizes the above comments. It's proof will be presented in details in our forthcoming paper.

Theorem 1. If $\alpha > b^2$, the external forcing $f(r,\theta,t)$ is sufficiently smooth, and $a < 1/c$, then there exists a unique solution $u \in C\left(\mathbb{R}^+, H_0^s(\Omega)\right)$, $s < 0$ of problem (4). The solution can be represented as

$$u(r,\theta,t) = \sum_{m\in\mathbb{Z}, n\in\mathbb{N}} \hat{u}_{mn}(t) J(\lambda_{mn} r) e^{im\theta}. \tag{17}$$

3 Numerical Results

In this section we apply the eigenfunction method described in the previous section in order to construct solutions numerically. We emphasize that (4) describes only *small* nonlinear oscillations of certain elastic membranes. Large nonlinear oscillations are described by the general Föppl–von Kármán system (derived by A. Föppl in 1907 [2] and analyzed by von Kármán in 1910 [13]). However, in order to test the convergence properties of the eigenfunction method, we use parameter values for which oscillation are relatively large, and hence the nonlinear term will have a prominent effect on the solution. We used parameter values $\alpha = 2$, $\beta = 100$, $a = 1000$ and $b = 0.1$ in our numerical analysis, with forcing term $f(r,\theta,t) = \delta(t)\cos(r\pi/2)$ for $t \geq 0$, $r \in [0,1]$ and $\theta \in [0, 2\pi]$, where δ is the Dirac Delta function (see, Fig. 1). After this initial "kick" the system undergoes nonlinear oscillation with small damping.

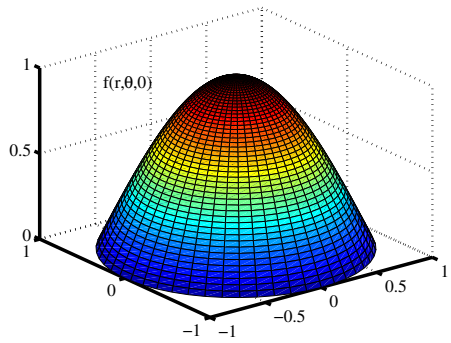

Figure 1. Initial forcing

Although these values are not realistic, they are appropriate for testing the numerical algorithm:

(1) $b = 0.1$, the damping is small, oscillations are strong.
(2) $\beta = 100$ is large, strong nonlinear effect.
(3) $a = 1000$ is large, shows that condition (16) for convergence of the method is a very conservative estimate.

We used FORTRAN90 with IMSL and CERNLIB subroutines for numerical calculations, and MATLAB 6.5 for visualization on a LINUX workstation with 2×2GHz processors and 2GB memory.

3.1 The Numerical Procedure

We describe in more details the numerical procedure that is based on the theoretical results of the previous section. We consider only real valued solutions, and hence we use cosine functions instead of the complex exponentials.

Although certain values related to special functions are tabulated in the literature, it is simpler and less prone to human errors if one calculates them through numerical approximations. One of these quantities are $\{\lambda_{mn}\}_{mn=01}^{MN}$, a truncated set of zeros for the Bessel functions, where M and N are positive integers. We used the CERNLIB subroutine DBZEJY in order to approximate these zeros. This subroutine uses an iterative method [10]. Another sequence of quantities consists of the squared L_2–norms of the eigenfunctions,

$$\left\{\|\Phi_{mn}\|^2\right\}_{m,n=0,1}^{M,N} = \int_0^{2\pi} \int_0^1 |\Phi_{mn}(r,\theta)|^2 \, r d\theta dr. \tag{18}$$

The method consists of the following main steps:

(1) Calculate the Fourier–Bessel coefficients of the forcing using formula

$$\hat{f}_{mn}(t) = \frac{< f, \Phi_{mn} >}{\|\Phi_{mn}\|^2} = \frac{\int_0^1 \int_0^{2\pi} f(r,\theta,t) J_m(\lambda_{mn} r) \cos(n\theta) \, r d\theta dr}{\int_0^1 \int_0^{2\pi} |\Phi_{mn}(r,\theta)|^2 \, r d\theta dr} \tag{19}$$

where $m = 0, \ldots M$ and $n = 1, \ldots, N$. The integrations in polar coordinates require discretization. We used

simple Riemann sums in polar coordinates with constant dr and $d\theta$ mesh sizes.

(2) Calculate the nonlinear coefficients

$$b(m,n,p,q,k,s) = \frac{<\Phi_{pq}\cdot\Phi_{ks},\Phi_{mn}>}{\|\Phi_{mn}\|^2} = \frac{\int_0^1\int_0^{2\pi} J_p(\lambda_{pq}r)J_k(\lambda_{ks}r)J_m(\lambda_{mn}r) \times\cos((p+k-m)\theta)\,r\,d\theta dr}{\int_0^1\int_0^{2\pi}|\Phi_{mn}(r,\theta)|^2\,r\,d\theta dr} \quad (20)$$

where $m=0,\ldots M$, $n=1,\ldots,N$. While there are a total number of $(M+1)^3N^3$ terms, due to orthogonality we have that $b(m,n,p,q,k,s)\neq 0$ only if $p+k=m$. This reduces the number of nonzero terms to $(M+1)^2N^3$. Further reduction in storage can be achieved by using the symmetry of the terms.

(3) Calculate the perturbation series recursively

$$\hat{v}_{mn}^{(0)}(t) = \frac{1}{\sigma_{mn}}\int_0^t e^{-b\lambda_{mn}^2(t-\tau)}\sin[\sigma_{mn}(t-\tau)] \times\hat{f}_{mn}(\tau)d\tau, \quad (21)$$

$$\hat{v}_{mn}^{(l)}(t) = -\frac{\beta\lambda_{mn}^2}{\sigma_{mn}}\int_0^t e^{-b\lambda_{mn}^2(t-\tau)}\sin[\sigma_{mn}(t-\tau)] \times\sum_{p,q,k,s} b(m,n,p,q,k,s)\sum_{j=1}^{l}\hat{v}_{pq}^{(j-1)}(\tau)\hat{v}_{ks}^{(l-j)}(\tau)d\tau \quad (22)$$

for $l=1,\ldots,N_v$, $t\in[0,T]$, $m=0,\ldots M$ and $n=1,\ldots,N$. This part is the most demanding computationally. It requires the evaluation of convolution type integrals and 5 sums embedded in the integral. We used Simpson's method for the approximation of the convolution with constant step size dt.

(4) Assemble the Fourier–Bessel coefficients of the solution

$$\hat{u}_{mn}(t) = \sum_{l=0}^{Nv} a^{l+1}\hat{v}_{mn}^{(l)}(t) \quad (23)$$

at all gridpoints t. This part is trivial.

(5) Assemble the solution

$$u(r,\theta,t) = \sum_{m=0}^{M}\sum_{n=1}^{N}\hat{u}_{mn}(t)J(\lambda_{mn}r)e^{im\theta} \quad (24)$$

at gridpoints t, r, θ.

3.2 Discretization Errors and Convergence Properties

A clear advantage of this method is that there is no modeling error involved. Errors are arising only in the discretization steps and from truncations of infinite series. The method has several of both steps. Below we examine the convergence properties of the method regarding these approximations.

A distinctive property of the method is that like a spectral method, by working in the Fourier–Bessel space the spatial discretization is present only in the initial (18)–(20) and final (24) phase of the algorithm. Also, there is no explicit numerical differentiation involved. The approximation of zeros $\{\lambda_{mn}\}_{m,n=0,1}^{M,N}$ can be done off–line and with virtually arbitrary high precision, hence we do not discuss that part.

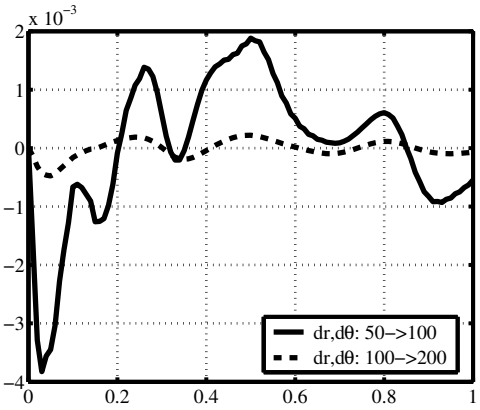

Figure 2. Spatial discretization error

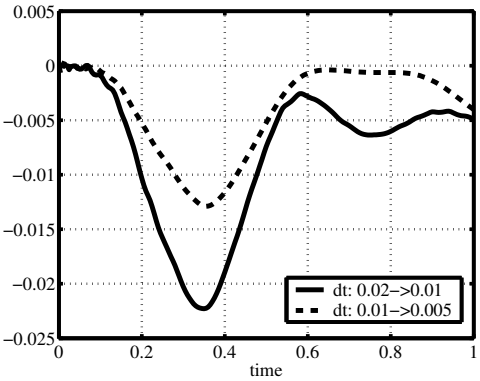

Figure 3. Time discretization error

In order to examine the convergence properties of solutions the sample point $(1/2,\pi)$ (half way between the center and the edge of the unit disk) was chosen. All the numerical values below were obtained at that point.

Spatial discretization Fig. 2 shows the convergence properties with respect to spatial discretization in terms of variables r and θ. The gridpoints are equally distributed in both directions.The change in the solution at the point is shown as the number of gridpoints was increased from 50 to 100 (solid line) and from 100 to 200 (dash line). Doubling the number of gridpoints lowered the change by almost one magnitude.

Time discretization In each time step we have to evaluate a convolution type integral, which includes the summation of $(M+1)^2N^3N_v$ terms. Fig. 3 shows the change in the solution as the time step is reduced from $dt=0.02$ to 0.01 and from 0.01 to 0.005. The convergence seem to be linear, and the figure shows the stability in time of the numerical method.

Convergence of the convolutive sum We examine now the convergence properties of the convolutive sum $\sum_{j=1}^{l}\hat{v}_{pq}^{(j-1)}\hat{v}_{ks}^{(l-j)}$, $l=1,\ldots,N_v$ in formula (22). The theoretical

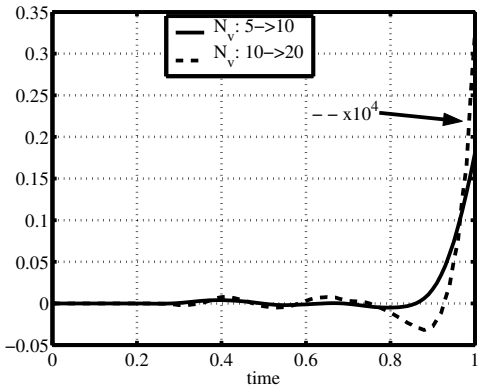

Figure 4. Convergence of the convolutive sum.

results of Section 2 are concentrated on the convergence properties of this iteration, and quadratic convergence has been established in (14) based on somewhat conservative estimates.

We increased N_v from 5 to 10 and then from 10 to 20. Fig. 4 shows that doubling the number of terms reduced the change in the solution by *four* magnitude. Solutions seem to diverge from each other in time, indicating that for larger time intervals one has to increase the number of iteration steps, N_v. This numerical finding is also in agreement with the theoretical results, as the convergence of the iteration was established for given finite time interval $[0,T]$. It is also important to note that the coefficient of the nonlinear term in (4) was chosen to be $\beta = 100$ which is an extremely high (non–physical) value. As a result the nonlinear dynamics dominates the solution, and hence it is natural that we have to take into consideration more nonlinear terms.

The number of basis functions The basis functions

$$\Phi_{mn}(r,\theta) = J_m(\lambda_{mn} r) e^{im\theta}$$

form a two–parameter family of orthogonal functions, where $m = 0,1,\ldots,M$ and $n = 1,2,\ldots,N$. We consider the cases $N = 5, 10, 15$ and $M = 5, 10, 15$. Due to the cubic factor N^3 in the number of coefficients $\{b(m,n,p,q,k,s)\}$ we were not able to complete the calculations in a reasonable amount of time for values of N larger than 15. Both cases show approximately a magnitude decrease in the change of the solution. The decrease in error is uniform in time when N, the number of zeros is increased. Large time solutions do not show dependence on the number of Bessel functions (M) used.

3.3 Nonlinear Oscillations

We present here two pictures of forced nonlinear oscillations of the membrane. Detailed analysis of the long time asymptotics will be presented in our forthcoming paper. In this example we use time varying forcing term $f(r,\theta,t) = \cos(r\pi/2)\sin(2\pi t)$ for $t \in [0,3]$, $r \in [0,1]$ and $\theta \in [0,2\pi]$. In this time varying case we had to lower the perturbation parameter to $a = 5$ in order to prevent the blow up of the

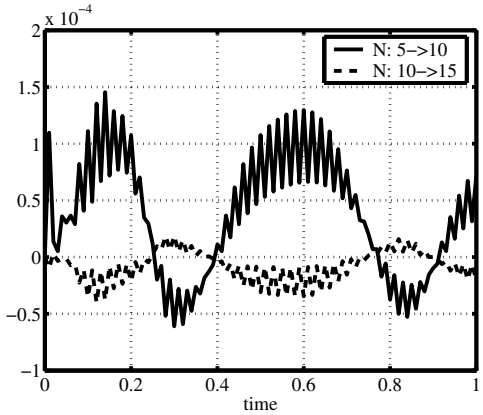

Figure 5. Convergence as the number of zeros is increased.

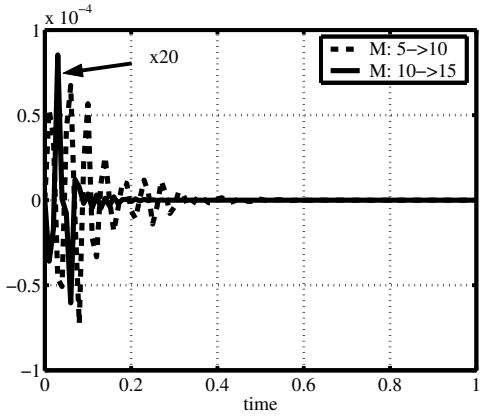

Figure 6. Convergence as the number of Bessel functions is increased.

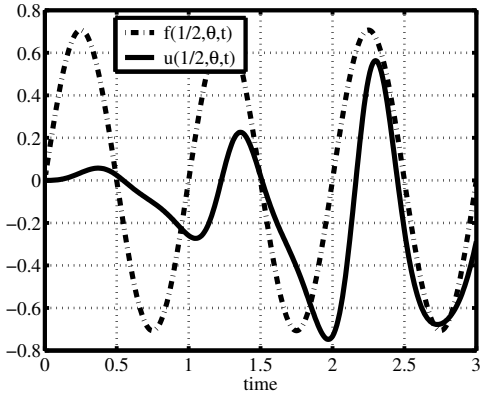

Figure 7. Forced nonlinear oscillations at a sample point

simulation, but this value is still much higher than the value 0.1 obtained by theoretical calculations. In Fig.7 we show the forced oscillation of a single sample point at $(1/2,\pi)$ along with the forcing at the same point. The oscillation of the membrane slowly takes on the frequency of the forcing. Fig. 8 shows the shape of the membrane at time $t = 2$.

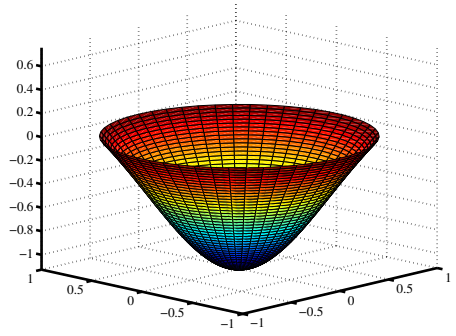

Figure 8. Forced oscillations of the membrane

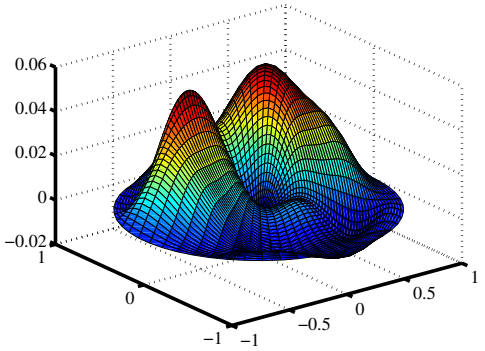

Figure 9. Nonlinear Oscillation with Small Damping at $t = 0.32$

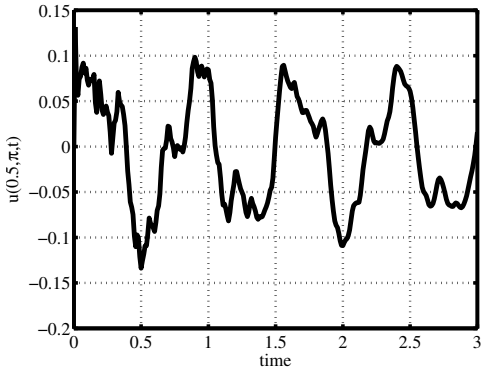

Figure 10. Nonlinear Oscillation with Small Damping.

3.4 Effect of Small Damping

Here we consider the case of small damping ($d = 0.01$) with the coefficient of the quadratic term having coefficient $\beta = 1000$. The forcing is restricted to an instantaneous delta function concentrated at $(r, \theta) = (0.5, \pi)$. Figure 9 shows highly nonsymmetric oscillations as a result of the nonsymmetric initial forcing. Figure 10 shows the very slow decay of the oscillations.

4 Conclusions and Future Works

The eigenfunctions expansion method was developed for a forced nonlinear Boussinesq equation representing forced, small and nonlinear oscillations of an elastic membrane. The method was used for numerical simulations. The numerical algorithm required several levels of approximations. All these steps were tested for convergence. The convergence properties show that the eigenfunction expansion is a viable alternative to other numerical methods.

In the future we plan to investigate the long time asymptotics of the nonlinear forced membrane oscillations for specific forcing functions. In order to describe large nonlinear oscillations of a membrane we are going to consider the general Föppl–von Kármán system [2].

5 Acknowledgments

The authors gratefully acknowledge the contribution of the Army Research Office.

References

[1] J. Bona and L. Luo, More Results on the Decay of Solutions to Nonlinear Dispersive Wave Equations, *Discrete and Continuous Dynamical Systems*, No. 1, 1995, pp151–193.

[2] A. Föppl, *Vorlesungen ü*, Technische Mechanik, Leipzig, 1907. Bd. 5.

[3] J.E. Gordon, *The Science of Structures and Materials*, Scientic American Books, 1988.

[4] T. Herzog, *Pneumatic Structures – a Handbook of Inflatable Architecture,* Oxford Univ. Press, New York, 1976.

[5] J. E. Lagnese, G. Leugering, and E.J.P.G. Schmidt. Modeling, Analysis and Control of Dynamic Elastic Link Structures. Birkhauser, Boston, 1994.

[6] J.E. Lagnese, *Boundary Stabilization of Thin Plates*, SIAM, Philadelphia, 1989.

[7] L.D. Landau and E.M. Lifshitz, *Theory of Elasticity*, Addison–Wesley, Inc., London, 1959.

[8] J.W. Lee R. B. Guenther, *Partial Differential Equations of Mathematical Physics and Integral Equations*, Prentice Hall, NJ, 1988.

[9] O.V. Rudenko and S.I. Soluyan, *Theoretical Foundations of Nonlinear Acoustics*, Moscow, Nauka, 1975.

[10] N.M. Temme. An Algorithm with Algol60 Program for the Computation of the Zeros of Ordinary Bessel Functions and those of their Derivatives, *J. Comput. Phys.*, No. 32, pp. 270–279, 1979.

[11] V. Varlamov, On the Initial–Boundary Value Problem for the Damped Boussinesq Equation, *Discrete Continuous Dynamical Systems*, Vol. 4, No. 3, pp. 431–444, 1998.

[12] V. Varlamov, On the Spatially Two–Dimensional Boussinesq Equation in a Circular Domain, *Nonlinear Analysis*, No. 46, pp. 699–725, 2001.

[13] Th. von Kármán, *Encyclopedia d. Math. Wiss.,* Lepzig, 1910. Bd. IV 2, II.

[14] N.J. Zabusky, *Nonlinear Partial Differential Equations*, Acad. Press, New York, 1967.